Time-Frequency Analysis of Nonlinear Systems: The Skeleton Linear Model and the Skeleton Curves

Lili Wang
e-mail: wllxxx@yahoo.com.cn
State Key Laboratory of Nonlinear Mechanics (LNM), Chinese Academy of Sciences, and Institute of Applied Physics and Computational Mathematics, Beijing, P.R. China

Jinghui Zhang

Chao Wang

Shiyue Hu

Civil College, Xi'an Jiaotong University, Xi'an, P.R. China

The joint time-frequency analysis method is adopted to study the nonlinear behavior varying with the instantaneous response for a class of S.D.O.F nonlinear system. A time-frequency masking operator, together with the conception of effective time-frequency region of the asymptotic signal are defined here. Based on these mathematical foundations, a so-called skeleton linear model (SLM) is constructed which has similar nonlinear characteristics with the nonlinear system. Two skeleton curves are deduced which can indicate the stiffness and damping in the nonlinear system. The relationship between the SLM and the nonlinear system, both parameters and solutions, is clarified. Based on this work a new identification technique of nonlinear systems using the nonstationary vibration data will be proposed through time-frequency filtering technique and wavelet transform in the following paper. [DOI: 10.1115/1.1545768]

1 Introduction

The identification of nonlinear systems has received considerable attention in recent years because most real structures exhibit some degree of nonlinearity. Various identification techniques have been proposed both in parametric method and nonparametric method. A good summary of the most relevant methods employed in dynamic testing is given in reference [1]. However, there is not a generally applicable one. For example, with the linearization method, apart from potential errors, there is a drawback of high variance in the predictions with different input and output data. With the higher order spectral analysis, there are problems of mathematical complexity, slow convergence rate, large storage requirements and extreme computation time. With the neural network which has been significantly advanced recently, in many actual cases we cannot obtain enough data to train the network. The nonlinear modal analysis is less than successful.

The dynamic behavior of a nonlinear system generally varies with the amplitude of its response. And many transient responses exhibit this variance in an inconspicuous way. The most successful approach to studying this varying dynamic nature is offered by the Hilbert transform. In reference [2,3], the nonlinear system is studied using a time-varying linear model called the pseudolinear one. The backbone curve and the instantaneous logarithmic decrement of the system are obtained to describe quantitatively the nonlinear behavior of the system through the Hilbert transform, the band-pass and low-pass filtering technique. But the bandwidth of the band-pass filter and the cut-off value of the low-pass filter have inexplicit physical interpretations and thus makes it not so facilitative in application. Later several attempts have been made to study the nonlinearity by using the time-frequency analysis method. The authors in [4,5] used the Wigner-Ville distribution, those in [6] used the Gabor transform, and those in [7,8] used the wavelet transform. All these references provide more effective identification procedures to study the nonlinear nature of instantaneous vibration characteristics.

In our work [9], the nonlinear system is studied based on the quadratic time-frequency distribution. The aim of this paper is to construct a mapping operator in time-frequency domain by which the nonlinear system is mapped to a linear model with changing coefficients. The relationship between the nonlinear system and the simple model, with consideration of their parameters, response and dynamic natures, is clarified systemically. This model indicates the nonlinear nature of the nonlinear system in a rather explicit way. Moreover, based on this modal, the parameters of the nonlinear system may be estimated from the nonstationary vibration data through a time-frequency filtering technique with high accuracy.

In section 2, the quadratic time-frequency distribution of the Cohen class is briefly introduced first. This is the necessary and important foundation for time-frequency analysis, especially to the newcomers in this area. Then a so-called time-frequency masking operator, together with the effective time-frequency region of the asymptotic signal are defined. Also two important conclusions are deduced. A class of nonlinear system is mapped to a time-varying linear system through the time-frequency masking operator in section 3. This time-varying linear system, which is called the skeleton linear model (denoted by SLM for a short) in this paper, has the similar dynamic behavior of the corresponding nonlinear one. The nature of the nonlinearity of the system may be indicated by the relationship between the instantaneous parameters and the instantaneous response of the SLM. And the response of the SLM is a sub-component of that of the nonlinear one. To describe the characteristics of the stiffness and damping in the nonlinear system in visual forms, the frequency skeleton curve and the damping skeleton curve are defined in section 4. The existence and the main nature of the nonlinearity can be seen at a glance of them.

The theory advanced here results in a new identification method through time-frequency filtering for nonlinear systems based on the measured nonstationary vibration data. The identification procedure will be discussed in detail in the subsequent paper.

2 Mathematical Foundation

2.1 The Quadratic Time-frequency Distribution of Nonstationary Signals. For an arbitrary time series, $x(t)$, we can always have its Hilbert transform, $\tilde{x}(t)$, as

Contributed by the Technical Committee on Vibration and Sound for publication in the JOURNAL OF VIBRATION AND ACOUSTICS. Manuscript received Sept. 2000; Revised Sept. 2002. Associate Editor: A. Vakakis.

$$\tilde{x}(t)=\frac{1}{\pi}PV\int_{-\infty}^{+\infty}\frac{x(\tau)}{t-\tau}d\tau \tag{1}$$

where PV indicates the Cauchy principal value. With this definition, $x(t)$ and $\tilde{x}(t)$ form a complex conjugate pair, so we can have an analytic signal, $X(t)$, as

$$X(t)=x(t)+j\tilde{x}(t)=a(t)e^{i\theta(t)} \tag{2}$$

in which

$$a(t)=\sqrt{x^2(t)+\tilde{x}^2(t)} \tag{3}$$

$$\varphi(t)=\arctan\frac{\tilde{x}(t)}{x(t)} \tag{4}$$

and we have

$$x(t)=a(t)\cos\varphi(t) \tag{5}$$

$$\tilde{x}(t)=a(t)\sin\varphi(t) \tag{6}$$

If there is

$$\frac{1}{a(t)}\left|\frac{da(t)}{dt}\right|\ll\left|\frac{d\varphi(t)}{dt}\right| \tag{7}$$

$x(t)$ or $X(t)$ is called an asymptotic signal. In the following part we can see that an asymptotic signal is with a narrow-band in the time-frequency plane at any given time. Its instantaneous frequency is $\omega(t)=d\varphi(t)/dt$, and its instantaneous band-width is $\Delta\omega(t)=1/a(t)|da(t)/dt|$.

For nonstationary signals, the commonly used signal processing methods based on the Fourier transform are not effective in which the signal is not expanded in both time and frequency domain. The Fourier spectrum gives only the signal's total strength at a certain frequency, but no time-localized information. The signal's instantaneous dynamic characters cannot be shown through the Fourier transform even if no information of the signal has been lost during the processing procedure.

Defined in the time-frequency domain, the joint time-frequency analysis method represents the one-degree time series with a two-degree function in the time-frequency plane. Tiny variance with time in the signal can be described through this method. In particular, the quadratic time-frequency distribution of Cohen class provides an effective way to describe the energy density in the time-frequency plane, which is defined as

$$\rho_x(t,\omega)=\frac{1}{4\pi^2}\int_{-\infty}^{+\infty}\int_{-\infty}^{+\infty}\int_{-\infty}^{+\infty}\phi(\theta,\tau)X^*\left(u-\frac{1}{2}\tau\right)\cdot X(u+\tfrac{1}{2}\tau)e^{-j\theta t-j\tau\omega+j\theta u}du\,d\tau\,d\theta \tag{8}$$

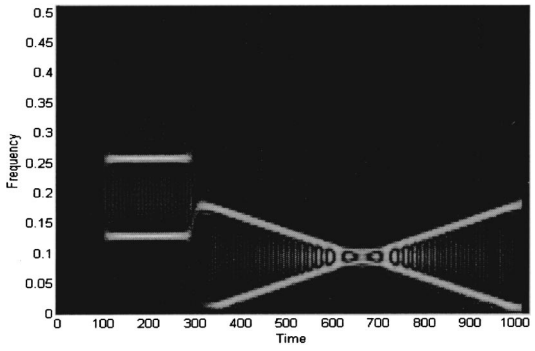

Fig. 1 Grayscale view of the modulus of quadratic time-frequency distribution of $x(t)$

where $\phi(\theta,\tau)$ is the kernel function of the quadratic time-frequency distribution. For more details on the Time-Frequency analysis, the reader is referred to reference [10].

The linear superposition principle is not valid for any quadratic time-frequency distributions. According to the definition (8) we have

$$\rho_{x_1+x_2}(t,\omega)=\rho_{x_1}(t,\omega)+\rho_{x_2}(t,\omega)+\rho_{x_1x_2}(t,\omega)+\rho_{x_2x_1}(t,\omega) \tag{9}$$

where $\rho_{x_1x_2}(x,t)$ and $\rho_{x_2x_1}(x,t)$ is called the cross-term.

Apparently the cross-term is without physical meaning. Generally, high time-frequency resolution and low cross-term are the most important factors we expect in constructing a quadratic time-frequency distribution. The Wigner-Ville distribution is not a good choice because the cross-term with it is too significant to be neglected. Here we use an exponential-cone-shaped kernel [11] which is expressed by

$$\phi(t,\tau)=\begin{cases}\dfrac{g(\tau)}{\sqrt{4\pi\tau^2/\sigma}}\exp\left[-\dfrac{t^2\sigma}{4\tau^2}\right] & |t|<\dfrac{|\tau|}{\alpha}\\ 0 & |t|\geqslant\dfrac{|\tau|}{\alpha}\end{cases} \tag{10}$$

where $g(\tau)$ is a weighting function, τ and α are adjustable parameters.

To test the performance of this distribution, we use the following nonstationary signal:

$$x(t)=\begin{cases}0 & t\leqslant 100\\ \cos(2\pi t/4)+\cos(2\pi t/8) & 101\leqslant t\leqslant 300\\ \cos\left[\dfrac{\pi}{2000}(0.5t-301)t\right]+\cos\left[\dfrac{\pi}{2000}(1024-0.5t)t\right] & 301\leqslant t\leqslant 1024\end{cases}$$

Fig. 1 shows that the exponential-cone-shaped kernel distribution is excellent with consideration of both time-frequency resolution and the cross-term. Different from the Fourier spectrum (shown as Fig. 2), the quadratic time-frequency distribution gives the legible local nature in both time domain and frequency domain. At a glance we see that the signal consists of two asymptotic components with constant frequency during $101\leqslant t\leqslant 300$, and two asymptotic components with increasing and decreasing instantaneous frequency during $301\leqslant t\leqslant 1024$ and has nothing when $t\leqslant 100$.

2.2 The Time-frequency Masking Operator and the Basic Properties. In this section, we define a time-frequency masking operator and the effective time-frequency region of the asymptotic signal. And two important theorems are deduced. These provide

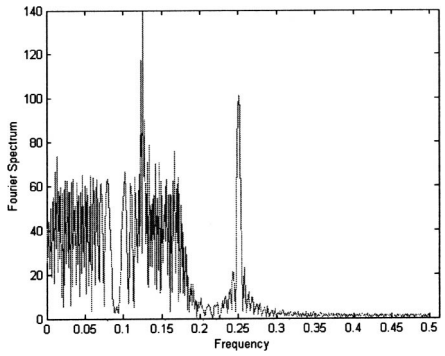

Fig. 2 The Fourier spectrum of $x(t)$

the mathematical foundation for the time-frequency analysis of nonlinear dynamic systems discussed in the next parts.

Definition 1:

Suppose $\rho_x(t,w)$ is the quadratic time-frequency distribution of a continuous signal $x(t)$, and Ω is a close region on the time-frequency plane

Let

$$\rho_x^{\Omega}(t,\omega)=\begin{cases}\rho_x(t,\omega) & (t,\omega)\in\Omega\\ 0 & (t,\omega)\notin\Omega\end{cases} \tag{11}$$

If the quadratic time-frequency distribution of a signal $y(t)$, $\rho_y(t,\omega)$, approximates $\rho_x^{\Omega}(t,\omega)$ best, we call $y(t)$ the projection of $x(t)$ on Ω, and the mapping from $x(t)$ to $y(t)$ the time-frequency masking operator on region Ω, denoted by

$$M(\cdot,\Omega):x(t)\rightarrow y(t) \tag{12}$$

Obviously $M(\cdot,\Omega)$ acts like a time-frequency filtering procedure with pass region Ω.

Definition 2:

The effective time-frequency region of the asymptotic signal $x(t)=a(t)\cos\varphi(t)$ is defined as

$$\Omega_x=\left[\omega(t)-\frac{\Delta\omega(t)}{2},\ \ \omega(x)+\frac{\Delta\omega(t)}{2}\right] \tag{13}$$

where

$$\omega(t)=\dot{\varphi}(t) \tag{14}$$

$$\Delta\omega(t)=\left|\frac{\dot{a}(t)}{a(t)}\right| \tag{15}$$

From the definition of the asymptotic signal, Eq. (7), we have

$$\Delta\omega(t)\ll\omega(t) \tag{16}$$

which means that the asymptotic signal is a narrow-band one in the time-frequency domain. The value of its instantaneous frequency changes from point to point in time.

Theorem 1:

Suppose $x(t)$ is an asymptotic signal with effective time-frequency region Ω_x. The projection of its continual function $f(x(t))$ on Ω_x can be approximated as

$$M[f(x(t)),\Omega_x]\approx\frac{1}{\pi}\left[\int_0^{2\pi}f(a\cos\varphi)\cos\varphi d\varphi\cdot\cos\varphi+\int_0^{2\pi}f(a\cos\varphi)\sin\varphi d\varphi\cdot\sin\varphi\right] \tag{17}$$

Proof:

$f(x(t))=f(a(t)\cos\varphi(t))$ is a function of time t. Because a varies slowly compared with $\cos\varphi$, it may be considered as a variable independent of φ. And we may take it for a constant within any period of $\cos\varphi$. Thus f may be considered as the function of two independent variables, a and φ. Besides, it is a pseudo-periodic function of φ with a slowly varying parameter a. Taking its Fourier series expansion about φ

$$f[x(t)]=f[a(t)\cos\varphi(t)]=\frac{C_0(t)}{2}+\sum_{n=1}^{+\infty}[C_k(t)\cos k\varphi(t)+D_k(t)\sin k\varphi(t)] \tag{18}$$

$$C_0(t)=\frac{1}{\pi}\int_0^{2\pi}f(a(t)\cos\varphi)d\varphi$$

$$C_k(t)=\frac{1}{\pi}\int_0^{2\pi}f(a(t)\cos\varphi)\cdot\cos k\varphi d\varphi \tag{19}$$

$$D_k(t)=\frac{1}{\pi}\int_0^{2\pi}f(a(t)\cos\varphi)\cdot\cos k\varphi d\varphi$$

In the above integrals, we take $a(t)$ for a variable independent of φ. Divide the time-frequency plane into pieces as follows:

$$\Omega^k(t,\omega)=\begin{cases}[0,\frac{1}{2}\omega(t)] & k=0\\ \left[\dfrac{2k-1}{2}\omega(t),\dfrac{2k+1}{2}\omega(t)\right] & k=1,2,3,\ldots\end{cases} \tag{20}$$

From (13), (16) and (20), it is obviously seen that $\Omega_x(t,\omega)\subset\Omega^1(t,\omega)$. And the central line of the two regions coincides with each other. The k-th order components, $C_k\cos k\varphi$ and $D_k\sin k\varphi$, are localized in a narrow zone at the central line of $\Omega^k(t,\omega)$ in the time-frequency plane. Therefore only the first-order components, $C_1\cos\varphi$ and $D_1\sin\varphi$, are located on $\Omega_x(t,\omega)$. Thus for the projection of $f[x(t)]$ on $\Omega_x(t,\omega)$, we have

$$\begin{aligned}M[f[x(t)],\Omega_x]&\approx M[f[x(t)],\Omega^1]\\&\approx C_1(t)\cos\varphi(t)+D_1(t)\sin\varphi(t)\\&=\frac{1}{\pi}\left[\int_0^{2\pi}f(a\cos\varphi)\cos\varphi d\varphi\cdot\cos\varphi+\int_0^{2\pi}f(a\cos\varphi)\sin\varphi d\varphi\cdot\sin\varphi\right]\end{aligned} \tag{21}$$

A continuous nonlinear function defined in a close region may be approximated with a polynomial at any required precision. So the power series is of very important value in the analysis of nonlinear dynamic systems. Consider the projection of the symmetric power series of an asymptotic signal on its effective time-frequency region, there is

$$M[|x|^n\cdot\mathrm{sign}(x),\Omega_x]\approx\frac{1}{\pi}\left[\int_0^{2\pi}a^n|\cos\varphi|^n\mathrm{sign}(\cos\varphi)\cos\varphi d\varphi\cdot\cos\varphi+\int_0^{2\pi}a^n|\cos\varphi|^n\mathrm{sign}(\cos\varphi)\times\sin\varphi d\varphi\cdot\sin\varphi\right] \tag{22}$$

Because

$$\int_0^{2\pi} a^n|\cos\varphi|^n\cdot\text{sign}(\cos\varphi)\cos\varphi d\varphi$$

$$=a^n\int_0^{2\pi}|\cos\varphi|^{n+1}d\varphi=2\sqrt{\pi}\,\frac{\Gamma\left(\frac{n}{2}+1\right)}{\Gamma\left(\frac{n+1}{2}+1\right)}a^n \tag{23}$$

$$\int_0^{2\pi} a^n|\cos\varphi|^n\cdot\text{sign}(\cos\varphi)\sin\varphi d\varphi=0 \tag{24}$$

We have

$$M[|x|^n\cdot\text{sign}(x),\Omega_x]\approx\frac{2}{\sqrt{\pi}}\,\frac{\Gamma\left(\frac{n}{2}+1\right)}{\Gamma\left(\frac{n+1}{2}+1\right)}a^n\cos\varphi$$

$$=\frac{2}{\sqrt{\pi}}\,\frac{\Gamma\left(\frac{n}{2}+1\right)}{\Gamma\left(\frac{n+1}{2}+1\right)}a^{n-1}x \tag{25}$$

Rewrite (25) as follows

$$M(|x|^n\cdot\text{sign}(x),\Omega_x)\approx\mu(n)a^{n-1}x \tag{26}$$

Where the definition of function $\Gamma(\cdot)$ may be found in reference [12]. $\mu(n)=2/\sqrt{\pi}[\Gamma(n/2+1)/\Gamma((n+1)/2+1)]$, is a constant dependent on n. Several terms that will be used commonly are listed as follows:

$$\mu(0)=\frac{4}{\pi},\quad \mu(1)=1,\quad \mu(2)=\frac{8}{3\pi},\quad \mu(3)=\frac{3}{4},$$

$$\mu(4)=\frac{32}{15\pi},\quad \mu(5)=\frac{5}{8},\ldots$$

Theorem 2:

Suppose $x(t)$ is an asymptotic signal with effective time-frequency region Ω_x. The projections of its first two order derivatives on Ω_x are

$$M[\dot{x}(t),\Omega_x]\approx\dot{x}(t)$$
$$M[\ddot{x}(t),\Omega_x]\approx\ddot{x}(t) \tag{27}$$

Proof:

$$\dot{X}(t)=[\dot{a}(t)+ja(t)\omega(t)]e^{j\varphi(t)} \tag{28}$$

$$\ddot{X}(t)=[\ddot{a}(t)-a(t)\omega^2(t)+2j\omega(t)a(t)+ja(t)\dot{\omega}(t)]e^{j\varphi(t)} \tag{29}$$

If $a(t)$ and $\varphi(t)$ are smooth nonoscillating signals, the variables in the brackets are slow signals compared with $e^{j\varphi(t)}$. So the instantaneous frequencies of $\dot{x}(t)$ and $\ddot{x}(t)$ equal to $\omega(t)$. And they are all located within Ω_x in the time-frequency plane. The desired result is established.

3 Time-Frequency Filtering and the Skeleton Linear Model (SLM)

Consider the following S.D.O.F. autonomous nonlinear system

$$m\ddot{y}+F(y,\dot{y})=0 \tag{30}$$

The response is an asymptotic signal with a changeless instantaneous frequency when the system is a linear one. Generally, the response is no longer an asymptotic signal but a multi-component one if there is nonlinearity in the system. But for weak nonlinear systems and some special systems such as many piecewise linear systems, there is one asymptotic component being dominant. We call this asymptotic signal the principal component in this paper, and express it as

$$x(t)=a(t)\cos[\varphi(t)] \tag{31}$$

whose instantaneous amplitude, $a(t)$, and instantaneous frequency, $\omega(t)=d\varphi(t)/dt$, can be calculated as follows

$$a(t)=\sqrt{x^2(t)+\tilde{x}^2(t)} \tag{32}$$

$$\omega(t)=\frac{x(t)\dot{\tilde{x}}(t)-\tilde{x}(t)\dot{x}(t)}{x^2(t)+\tilde{x}^2(t)} \tag{33}$$

where $\tilde{x}(t)$ is the Hilbert transform of $x(t)$. $a(t)$ and $\omega(t)$ are variables varying slowly with time.

The response signal of (30) can be expressed as

$$y(t)=x(t)+z(t) \tag{34}$$

Where $z(t)$ is the residual signal including the sub-harmonic and super-harmonic components of $x(t)$. $z(t)$ and its derivatives are of much lower energy compared with $x(t)$ and its derivatives.

We use the following Duffing equation to illustrate the time-frequency behavior of the response signal.

$$\ddot{y}+0.05\dot{y}+\pi^2\cdot(0.2y+8y^3)=0$$

$$y(0)=2,\ \dot{y}(0)=0,\ \ddot{y}(0)=0$$

The nonlinearity in this system is rather significant. The Fourier Spectrum and modulus of the quadratic time-frequency distribution of $y(t)$ at $t=0\sim204.8$ are plotted in Figs. 3 and 4. The Fourier Spectrum shows that $y(t)$ is a signal with a broad band. But through the quadratic time-frequency distribution we see that in fact $y(t)$ is a quite simple asymptotic signal with an instantaneous frequency decreasing with time.

Now consider the projection of Eq. (30) on Ω_x, there is

$$M(m\ddot{x}+m\ddot{z}+F(x+z,\dot{x}+\dot{z}),\Omega_x)=0 \tag{35}$$

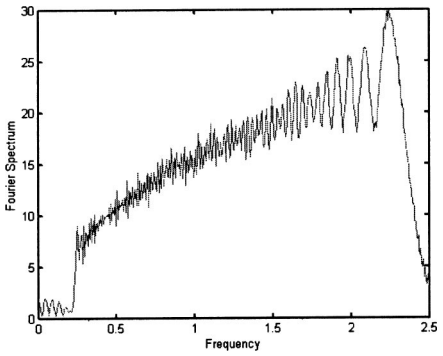

Fig. 3 The Fourier spectrum

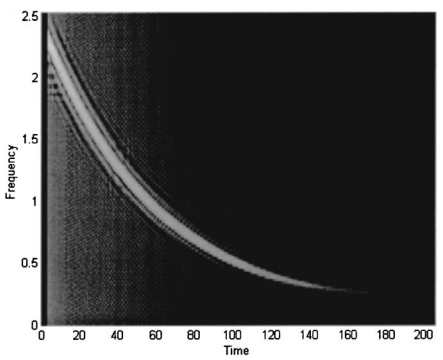

Fig. 4 The quadratic time-frequency distribution

$$M(z,\Omega_x)=M(\dot{z},\Omega_x)=M(\ddot{z},\Omega_x)=0 \tag{36}$$

For the projection of $F(x+z,\dot{x}+\dot{z})$ on Ω_x, except from those terms derived from $x(t)$, only a very little fraction of the nonlinear terms associated with $z(t)$ and its derivatives have the possibility to be nonzero. If $z(t)$ is the infinitesimal of $x(t)$, these terms are also the infinitesimal of $x(t)$, or the infinitesimal with high orders. Neglecting the contributions of $z(t)$ and its derivatives in $M(F(x+z,\dot{x}+\dot{z}),\Omega_x)$, one has

$$M(m\ddot{x}+F(x,\dot{x}),\Omega_x)=0 \tag{37}$$

Substituting (21), (27) to (37), it is deduced that the principal component $x(t)$ satisfies the following differential equation approximately

$$\ddot{x}+2h_0\dot{x}+\omega_0^2 x=0 \tag{38}$$

where

$$\omega_0=\left[\frac{1}{\pi m a}\int_0^{2\pi}F(a\cos\varphi,-a\omega\sin\varphi)\cos\varphi d\varphi\right]^{1/2} \tag{39}$$

$$h_0=-\frac{1}{2\pi m a\omega}\int_0^{2\pi}F(a\cos\varphi,-a\omega\sin\varphi)\sin\varphi d\varphi \tag{40}$$

This is a linear system with coefficients ω_0 and h_0 varying slowly with time. Its response is the principal component of that of system (30). And its instantaneous coefficients versus its instantaneous response indicate the nonlinear behavior of system (30) in a rather distinct way. So we call this time-varying linear system the skeleton linear model of system (30) and denote it by SLM for a short. ω_0 and h_0 are called the instantaneous undamped inherent frequency and the instantaneous decay coefficient of SLM, respectively.

For a S.D.O.F. nonlinear nonautonomous systems excited by an asymptotic signal, if the harmonic component is dominant in the response signal, its SLM has the same expression as (38)–(40). It should be noted that (38)–(40) is usually no longer valid if the harmonic component is not dominant in the response.

The model proposed here is of the same form with the quasi-linear system used in reference [2], [3]. In [2,3], the quasi-linear system is used for the parameter identification of nonlinear systems with no illumination about the relationship between the two systems. And the identification procedure is based on the Hilbert transform and the classical filtering technique. In this paper the SLM is deduced directly from the nonlinear system through the time-frequency masking operator based on the quadratic time-frequency distribution. The relationship between SLM and the corresponding nonlinear system, both about their parameters and their instantaneous response, is clarified systemically. Furthermore, the theory proposed here results in a time-frequency filtering technique for the parameter identification of nonlinear systems. The response signal of SLM may be accurately extracted from that of the corresponding nonlinear system by using the time-frequency filtering technique. Because response data of both the SLM and the nonlinear system are nonstationary signals, the extracted result is not accurate if we use the classical processing techniques based on the Fourier transform.

4 The Skeleton Curves

Equation (39) describes the main nature of the stiffness versus the response, while (40) describes that of the damping. Equations (39) and (40) represent two surfaces. With a measured experimental data, we could obtain two curves located on the two surfaces respectively. We call them *the frequency skeleton curve and the damping skeleton curve* of system (30), respectively. They give quantitative information about the existence and main nature of the nonlinearity in the system in visual forms.

For some systems, (39) and (40) have more compact expressions. Consider a system with the following form

$$m\ddot{y}+P(y)+Q(\dot{y})=0 \tag{41}$$

where $P(y)$ and $Q(\dot{y})$ are real-valued odd functions of y and $\dot{y}$, respectively. The instantaneous parameters of the SLM are

$$\omega_0(a,\omega)=\omega_0(a)=\left[\frac{1}{\pi a m}\int_0^{2\pi}P(a\cos\varphi)\cos\varphi d\varphi\right]^{1/2} \tag{42}$$

$$h_0(a,\omega)=h_0(a\omega)=-\frac{1}{2\pi a\omega m}\int_0^{2\pi}Q(-a\omega\sin\varphi)\sin\varphi d\varphi \tag{43}$$

In this case the two skeleton curves have only one independent variable, a or $a\omega$. Obviously, they are both horizontal straight lines for a linear system. The stiffness nonlinearity or the damping nonlinearity exists whenever the corresponding skeleton curve is not a horizontal straight line.

Suppose that $P(\cdot)$ and $Q(\cdot)$ are polynomials, Eq. (30) becomes

$$m\ddot{y}+\sum_{j=1}^{n}c_i|\dot{y}|^j\cdot\mathrm{sign}(\dot{y})+\sum_{i=1}^{m}k_i|y|^i\cdot\mathrm{sign}(y)=0 \tag{44}$$

according to (25), the skeleton curves are

$$\omega_0(a)=\left[\sum_{i=1}^{m}\frac{2}{\sqrt{\pi}m}\frac{\Gamma\left(\frac{i}{2}+1\right)}{\Gamma\left(\frac{i+1}{2}+1\right)}k_i\cdot a^{i-1}(t)\right]^{1/2}$$
$$=\left[\sum_{i=1}^{m}\frac{\mu(i)k_i}{m}\cdot a^{i-1}(t)\right]^{1/2} \tag{45}$$

$$h_0(a\omega)=\sum_{j=1}^{n}\frac{1}{\sqrt{\pi}m}\frac{\Gamma\left(\frac{j}{2}+1\right)}{\Gamma\left(\frac{j+1}{2}+1\right)}c_j\cdot[a(t)\omega(t)]^{j-1}$$
$$=\sum_{j=1}^{n}\frac{\mu(j)}{2m}c_j\cdot[a(t)\omega(t)]^{j-1} \tag{46}$$

Now we discuss the skeleton curves of some typical nonlinear systems.

(1) System with Nonlinear Spring

A spring is called a hard one if the stiffness coefficient increases with the displacement, and a soft one if the stiffness coefficient decreases when the displacement increases. Neglecting the hysteresis during the load and unload process, the relationship between the elastic force and displacement can be expressed as

$$P(y)=k_1y+k_2|y|y+\ldots k_n|y|^{n-1}y \tag{47}$$

the frequency skeleton curve is

$$\omega_0=\frac{1}{\sqrt{m}}[\mu(1)k_1+\mu(2)k_2a+\mu(3)k_3a^2+\ldots$$
$$+\mu(n)k_na^{n-1}]^{1/2}$$
$$=\frac{1}{\sqrt{m}}\left[k_1+\frac{8}{3\pi}k_2a+\frac{3}{4}k_3a^2+\ldots+\mu(n)k_na^{n-1}\right]^{1/2} \tag{48}$$

Where $\mu(\cdot)$ is defined in section 2. For systems with a soft spring, there is $k_i<0, i=2,\ldots,n$. The instantaneous undamped inherent frequency of SLM is a monotone decreasing function of a. For systems with hard spring, there is $k_i>0, i=2,\ldots,n$, So the instantaneous undamped inherent frequency of SLM is a monotone increasing function of a.

Consider the following system as an example:

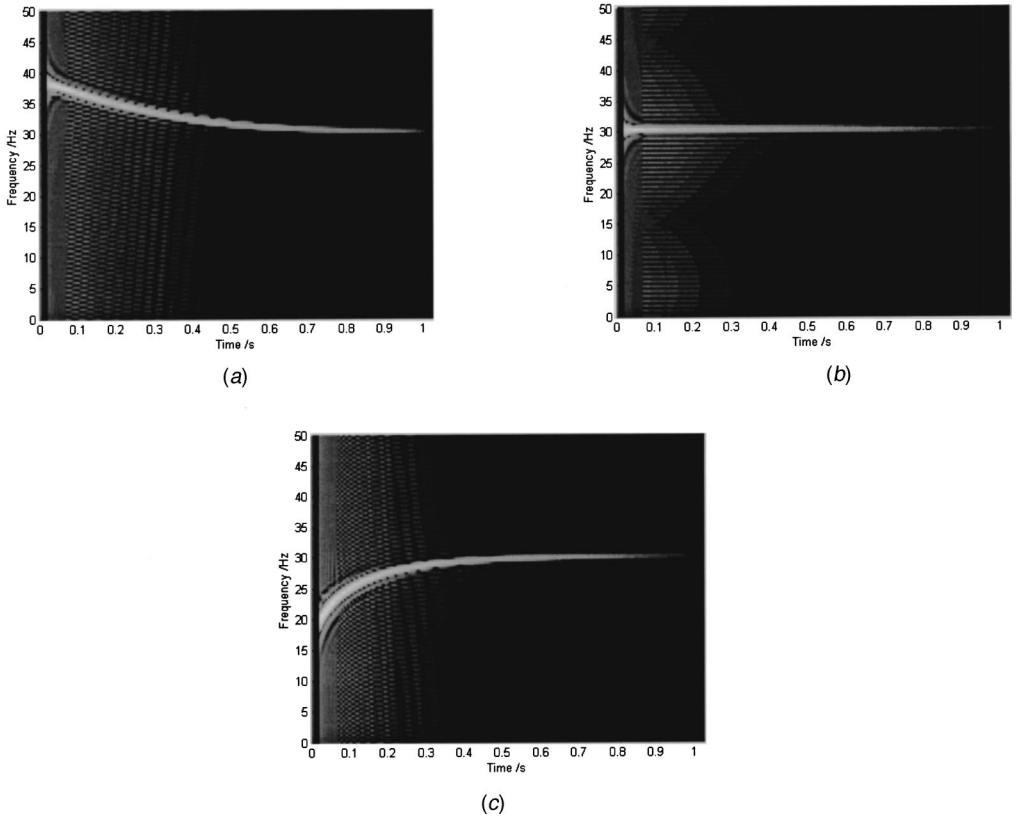

Fig. 5 The quadratic time-frequency distribution of $y(t)$ (*a*) α=200 (*b*) α=0 (*c*) α=−200

$$\ddot{y}+0.5\dot{y}+(2\pi)^2\times(900y+\alpha y^3)=0$$

$$y(0)=2,\quad \dot{y}(0)=0,\quad \ddot{y}(0)=0$$

Figure 5 shows the quadratic time-frequency distribution of $y(t)$ at α=200, 0, −200. For a linear spring with α=0, the instantaneous frequency of response $y(t)$ is a constant. For a nonlinear system with a hard spring, the instantaneous frequency of $y(t)$ decreases with time due to the amplitude decay, shown as Fig. 5(*b*). And for a soft spring, it takes the contrary. Figure 6 shows the elastic force versus the displacement. And the frequency skeleton curve is plotted in Fig. 7.

(2) System with Liquid Damping

When an object moves in liquid at large Reynolds number, the resistance is usually in direct proportion to the n-th power of the velocity. The model with a square damping, shown as Fig. 8, is a widely used one.

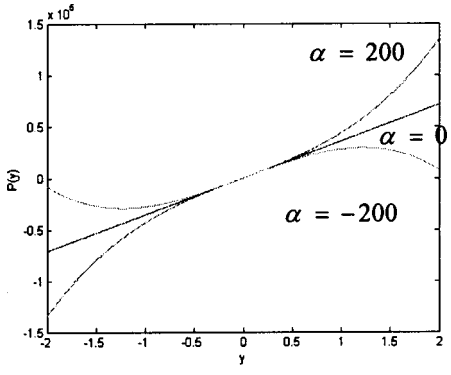

Fig. 6 The elastic force versus displacement

$$m\ddot{y}+ky+\eta|\dot{y}|\dot{y}=0 \tag{49}$$

the damping skeleton curve is

$$h_0(a\omega)=\frac{4\eta}{3\pi m}a\omega \tag{50}$$

which is a straight line shown as Fig. 9.

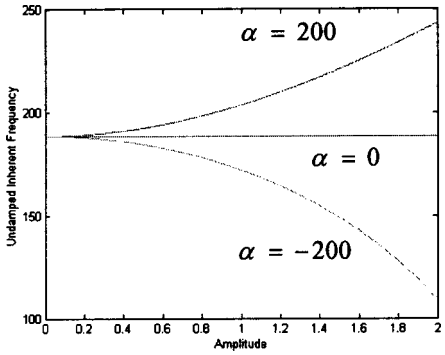

Fig. 7 The frequency skeleton curve

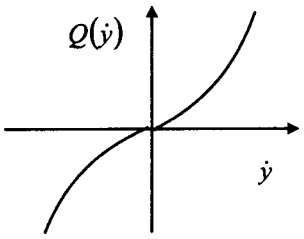

Fig. 8 Damping versus velocity in a system with square damping

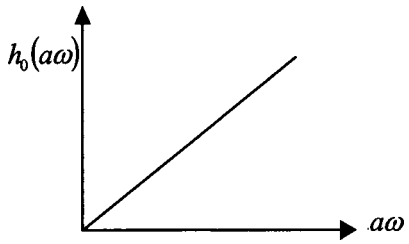

Fig. 9 Damping skeleton curve of a system with square damping

The nonlinear damping affects the instantaneous bandwidth of the response. It has no effect on the instantaneous frequency.

(3) Piecewise Linear System

Although a piecewise linear system is usually considered as one with a high degree of nonlinearity, its instantaneous response is always an asymptotic signal. So the SLM constructed here is valid for these systems. The skeleton curves of some typical piecewise linear systems deduced from Eq. (39) or (40) are listed here.

(A) Spring with a Backlash

$$P(y)=\begin{cases} k(y-\text{sign}(y)y_0) & |y|>y_0 \\ 0 & |y|\leqslant y_0 \end{cases} \tag{51}$$

where y_0 is the backlash in the spring. The frequency skeleton curve is

$$\omega_0(a)=\begin{cases} \sqrt{\dfrac{k}{m}-\dfrac{2k}{\pi m}\left[\sin^{-1}\dfrac{y_0}{a}+\dfrac{y_0}{a}\sqrt{1-\left(\dfrac{y_0}{a}\right)^2}\right]} & a>y_0 \\ 0 & a\leqslant y_0 \end{cases} \tag{52}$$

$$\omega_0(a)=\begin{cases} \sqrt{\dfrac{k_2}{m}+\dfrac{2(k_1-k_2)}{\pi m}\left(\sin^{-1}\left(\dfrac{y_0}{a}\right)+\dfrac{y_0}{a}\sqrt{1-\dfrac{y_0^2}{a^2}}\right)} & a\geqslant y_0 \\ \sqrt{\dfrac{k_1}{m}} & a<y_0 \end{cases} \tag{56}$$

Apparently there is:

$$\lim_{a\to\infty}\omega_0(a)=\sqrt{\frac{k_2}{m}}$$

(D) Elasticity Saturation

$$P(y)=\begin{cases} ky & |y|\leqslant y_0 \\ \text{sign}(y)\cdot ky_0 & |y|>y_0 \end{cases} \tag{57}$$

The frequency skeleton curve is

$$\omega_0(a)=\begin{cases} \sqrt{\dfrac{2k}{\pi m}\left(\sin^{-1}\left(\dfrac{y_0}{a}\right)+\dfrac{y_0}{a}\sqrt{1-\dfrac{y_0^2}{a^2}}\right)} & a\geqslant y_0 \\ \sqrt{\dfrac{k}{m}} & a<y_0 \end{cases} \tag{58}$$

Apparently there is:

$$\lim_{a\to\infty}\omega_0(a)=\sqrt{\frac{k}{m}}$$

(B) Pre-Compressed Spring

$$P(y)=\begin{cases} ky+F_0\cdot\text{sign}(y) & |y|\neq 0 \\ 0 & |y|=0 \end{cases} \tag{53}$$

where F_0 is the pre-compressive stress. The frequency skeleton curve is

$$\omega_0(a)=\sqrt{\frac{k}{m}+\frac{4F_0}{\pi am}} \tag{54}$$

Apparently there is:

$$\lim_{a\to\infty}\omega_0(a)=\sqrt{\frac{k}{m}}$$

$$\lim_{a\to 0}\omega_0(a)=\infty$$

(C) Bi-Linear Spring

$$P(y)=\begin{cases} k_1y & |y|\leqslant y_0 \\ k_2y+\text{sign}(y)\cdot(k_1-k_2)y_0 & |y|>y_0 \end{cases} \tag{55}$$

The frequency skeleton curve is

$$\lim_{a\to\infty}\omega_0(a)=0$$

(E) Spring and Rigid Boundary

$$P(y)=\begin{cases} +\infty & y>y_0 \\ ky & |y|\leqslant y_0 \\ -\infty & y<-y_0 \end{cases} \tag{59}$$

The frequency skeleton curve is

$$\omega_0(a)=\begin{cases} +\infty & a\geqslant y_0 \\ \sqrt{\dfrac{k}{m}} & a<y_0 \end{cases} \tag{60}$$

(F) Coulomb Friction

$$Q(\dot{y})=\mu T\cdot\text{sign}(\dot{y}) \tag{61}$$

where μ is the friction coefficient. T is the normal pressure acted on the contact interface. The damping skeleton curve is

$$h_0(a\omega)=\frac{2}{\pi m}\mu T\cdot[a\omega]^{-1} \tag{62}$$

5 Conclusions

Based on the joint time-frequency analysis method, the skeleton linear model (SLM) is constructed for a class of nonlinear system. Solution of the SLM is the dominant sub-component in that of the nonlinear system. It may be extracted from the response data of the nonlinear system through the time-frequency masking operator defined in this paper. The relationship between the SLM's coefficients and the parameters in the corresponding nonlinear system is deduced, as shown as Eqs. (39) and (40). The SLM remains the main nonlinear behavior of the nonlinear system. Characteristics of the stiffness and damping of the nonlinear system may be described quantificationally with the frequency skeleton curve and damping skeleton curve.

The analysis advanced in this paper results in a new identification method based on the nonstationary vibration data. The identification procedure will be discussed in detail in the subsequent paper.

References

[1] Imregun, M., 1998, ''A Survey of Non-linear Analysis Tools for Structural Systems,'' Shock Vib. Dig., **30**(5), pp. 363–369.

[2] Feldman, M., 1994, ''Non-linear System Vibration Analysis Using Hilbert Transforml. Free Vibration Analysis Method 'Freevib','' Mech. Syst. Signal Process., **8**(2), pp. 119–127.

[3] Feldman, M., 1994, ''Non-linear System Vibration Analysis Using Hilbert TransformII. Forced Vibration Analysis Method 'Forcevib','' Mech. Syst. Signal Process., **8**(3), pp. 309–318.

[4] Feldman, M., and Braun, S., 1995, ''Identification of Non-linear System Parameters Via the Instantaneous Frequency: Application of the Hilbert Transform and Wigner-Ville Techniques,'' *Proc., of 13th IMAC*, Nashville, TN, pp. 637–642.

[5] Brancaleoni, F., Spina, D., and Valente, C., 1993, ''Damage Assessment from the Dynamic Response of Deteriorating Structures,'' *Safety Evaluation Based Identification Approaches*, Natke H. G., Tomlinson G. R., and Yao J. T. P., eds., Braunschweig.

[6] Spina, D., Valente, C., and Tomlinson, G. R., 1996, ''A New Procedure for Detecting Non-Linearity From Transient Data Using Gabor Transform,'' Nonlinear Dyn., **11**, pp. 235–254.

[7] Robertson, A. N., Park, K. C., and Alvin, K. F., 1995, ''Extraction of Impulse Response Data Via Wavelet Transform for Structural System Identification,'' *Proceedings of The Design Engineering Technical Conference*, ASME, **84**(1), pp. 1335–1344.

[8] Hyang, S. Y., Qi, G. Z., and Yang, J. C., 1994, ''Wavelets for System Identification,'' *Proc., of 12th IMAC*, Honolulu, HI, pp. 1162–1166.

[9] Wang, L., 1999, ''The Time-frequency Analysis of Dynamic Systems and its Applications in Non-linear Modelling,'' Ph.D. thesis, Xi'an Jiaotong Univ. P.R. China.

[10] Cohen, L., 1995, *Time-Frequency Analysis: Theory and Applications*, Prentice Hall.

[11] Liu, G., and Liu, Z., 1996, ''A New Quadratic Time-Frequency Distribution and a Comparative Study of Several Popular Quadratic Time-Frequency Distributions,'' J. Electron., **18**(5), pp. 455–461.

[12] Andrews, G. E., Askey, R., and Roy, R., 1999, *Special Functions*, Cambridge University Press, Cambridge.